Satellite Remote Sensing Activities for Earth Observation

Ana Vidal, Berta Hoyos, Mercé Llopis, Mariola Montoliu, Mª Rocío Moreno, Máriam Taroncher, Vicente E. Boria
Instituto de Telecomunicaciones y Aplicaciones Multimedia (iTEAM)
Universidad Politécnica de Valencia
Building 8G, access D, Camino de Vera s/n 46022 Valencia (SPAIN)
Corresponding author: avidal@dcom.upv.es

Abstract

Earth Observation by using Remote Sensing satellite data has become a very interesting technique for a wide variety of applications. The principal areas that demand this kind of data proceed from the government and military agencies, private companies or scientific organizations. This is the reason for the wide deployment of all a variety of remote satellite sensors mounted on a high number of satellites launched recently. New satellites include a broad range of spatial and spectral characteristics. Now, submeter spatial resolution can be obtained using commercial panchromathic optical sensors, and one-meter resolution is available in microwave radar imaging. These new products pave the way for the development of promising applications in different fields. This paper offers a review of the available satellite imagery, and it also describes recent research activities related to this field.

Keywords. Remote Sensing, Earth Observation, Synthetic Aperture Radar, SAR Processing, Speckle Noise, Image Classification, Land Use, Crop Identification, Irrigation Detection, Multi-temporal Classification.

1. Introduction

Earth Observation is an area of great interest and investment. Nowadays, commercial satellite imagery in the submeter range is already available with limited spectral resolution (1 or 4 bands) coming from several platforms like Ikonos/Geoeye and Quickbird/Worldview [1]. On the other hand, other instrumentation like the Advanced Spaceborne Thermal Emission and Reflection Radiometer (ASTER) onboard the scientific TERRA satellite (USA/Japan) with very good spectral resolution is also available. The sensor ASTER has three different subsystems, VNIR (visible and near infrared) with 15 m of pixel size, SWIR (infrared) with 30 m and TIR (thermal) with 90 m of pixel size. These sensors are only an example of optical products among many other possibilities such as the Landsat and the Spot programs which operate in the range of 20-30 m of pixel size. All these missions provide a huge field of potential practical applications. In this paper, per pixel classification for crop characterization and irrigation detection using ASTER data, and per object classification using aerial images that share resolution details with the submeter optical satellite imagery, are introduced.

Concerning the microwave spectrum, governments and space agencies are investing a great amount of effort in developing spaceborne platforms that carry Synthetic Aperture Radar (SAR) systems. These instruments are becoming a very important source of information for Earth Observation. Some of the most relevant programs are ERS, ENVISAT and the future Sentinel missions (ESA), Radarsat (Canada) and TerraSAR-X (Germany) (see [1] and [2]). The last program operates in the X band, and consequently it can provide very high resolution imagery (from 1 m to 30 m depending on the acquisition mode). In this paper, a study about SAR processing algorithms and Speckle noise reduction is described. SAR instruments produce a great amount of data to be stored that have been traditionally processed on ground. However, technological developments concerning microprocessors and solid state memories now enable the possibility of on-board SAR data processing (see [3] and [4]). In this scenario, efficient algorithms for generating SAR images are demanded. This new situation requires specially designed algorithms for the processing stages because high resolution approaches to SAR image generation are still too computationally expensive.

This paper describes the Remote Sensing activities carried out with the aforementioned products. First, microwave active remote sensing activities for image formation and restoration are described, then optical instrumentation applica-

Nowadays, commercial satellite imagery in the submeter range is already available.

tions are introduced and finally, classification and data fusion are considered as current trends.

2. Microwave Remote Sensing

SAR has played a very important role in the field of Earth Observation. It provides with valuable products to the scientific community like interferometric and polarimetric data (see [1] and [5]). The main advantages of satellite SAR systems are continuity, global monitoring of the Earth surface and operation under all weather and illumination conditions [2]. Besides, SAR data have shown a great potential exploited together with information coming from other instruments (visible and thermal bands) in the form of fusion algorithms. When compared to optical data, SAR images give apparently much noisier products, but they offer very valuable additional information that is not present in the optical range like man made structures and soil moisture characterization. There are also some other features that are much better characterized using microwave imaging that fall out of the scope of this paper like maritime oil spills and ice.

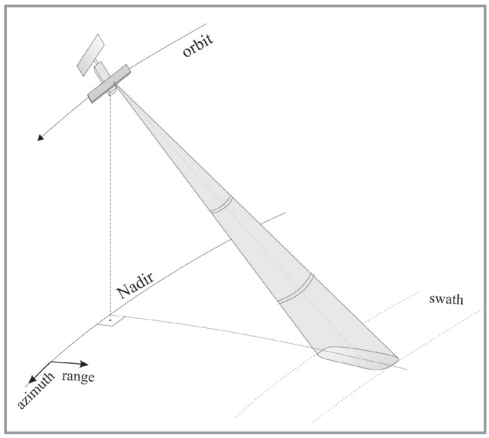

Figure 1. *SAR system geometry.*

The requirements of wide swaths for global monitoring, taking into account the geometry of the SAR system and its restrictions, have caused the development of the Scanning SAR technique (ScanSAR). In this mode of operation, the antenna beam is automatically and periodically steered in order to get several subswaths in one pass (this mode is supported in ENVISAT, RADARSAT and TerraSAR-X). Fig. 1 presents the acquisition geometry for a SAR system and Fig 2. describes the scanning mechanism in the ScanSAR system.

SAR focusing stages are usually carried out digitally by ground powerful computers (see [2]). However, recent advances in space qualification for efficient and programmable microprocessors bring the possibility of on-board SAR processing (see [3] and [4]). Only limited computing resources are expected in the first on-board processing systems and consequently, just reduced resolution images can be generated. Besides, reduced resolution decreases the amount of data to be downlinked and that fact is very important, since high data rates are one of the most restrictive drivers in SAR system design. In this context, there is a need of advanced algorithms capable to process medium resolution SAR and ScanSAR data. Efficient and modest algorithms are also very interesting due to their computational benefits for fast image generation. The scenario where this kind of algorithms could be appreciated would be on-board ScanSAR imaging or ground image generation for browsing purposes before high precision processing takes place (see [3] and [4]).

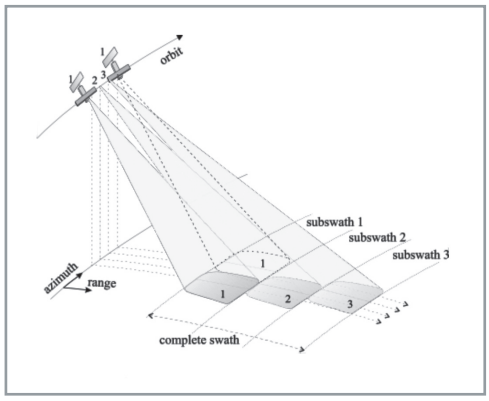

Figure 2. *ScanSAR system geometry.*

3. Range and azimuth processing

The Chirp signal used in SAR is usually a pure quadratic phase with a rectangular envelope modulated on a radio-frequency tone (usually in L, C or X bands). These pulses are sent to the surface and their echoes are sampled and recorded on board, and this constitutes the range dimension information that is stored in files. Then, matched filtering is carried out to recover the surface information on ground. This filtering may be practically implemented by several techniques (see [2] and [4]).

On the other hand, the system introduces an azimuth hyperbolic phase caused by the varying relative position between the target and the antenna. Besides, the antenna radiation pattern modulates the azimuth signal amplitude in the spectral domain. This signal is sampled by the Pulse Repetition Frequency (see [2]).

This paper presents a study among medium resolution processing algorithms that should able to process medium resolution SAR data as well as ScanSAR. The Range-Doppler algorithm using Fast Frequency Convolution is one of the most widely used methods and it is a good reference for comparison. It carries out matched filtering by fast convolution in the frequency domain, and its main drawback is the demanded Fast Fourier Transform (FFT) block size. Unfocused Synthetic Aperture algorithm (Unfocused SA) is a special kind of azimuth SAR processing [2] that

	UNFOCUSED SA	SPECAN-1D	SPECAN-2D	CZT-2D
ISLR (dB)	-33.37	-31.14	-32.57	-30.7
Range spatial resolution (pixels)	1.26	1.25	1.4	1.04
Azimuth spatial resolution (pixels)	1.28	1.26	1.25	0.9
Mean ENL in uniform zones	22.7	28.33	33.66	22.9

Table 1. *Medium resolution algorithm quality analysis.*

There is a need of advanced algorithms capable to process medium resolution SAR and ScanSAR data.

does not fully exploit the phase content of the synthetic aperture and it is not usually applied to range processing.

Spectral Analisys (SPECAN) (see [4], [6] and [7]) was introduced some years ago to process Chirp signals. The underlying theory is to implement a SAR processing algorithm by deramping and spectrum analysis. It is based on a quadratic phase model for the SAR signal. Hence, it may be applied for range compression [6] if a pure quadratic Chirp is used, and it can also be applied to azimuth processing if the azimuth phase history is sufficiently modelled with the second order term of the Taylor expansion [2]. However, SPECAN does not bring a satisfactory solution for ScanSAR data even with a proper selection of FFT size, because algorithms must make use of interpolation in order to get samples at the appropriate frequency positions. In range compression, it is also interesting to get an algorithm with freely selectable decimation factor in order to obtain a uniform image from the different swaths. Chirp Z-Transform SPECAN (CZT SPECAN) introduced by Vidal-Pantaleoni and Ferrando in [6] gives a much more flexible algorithm. Its decimation choice does not depend so critically on the system characteristics.

This new spectral analysis technique is a natural interpolator like the Chirp Scaling Algorithm, and for that reason is a very valuable tool for designing efficient algorithms avoiding interpolators.

This work compares in Table I different algorithms for medium resolution SAR processing: the Unfocused algorithm, SPECAN in azimuth, SPECAN for both azimuth and range and CZT-SPECAN in both azimuth and range. Overall processing evaluation is validated using ERS-1 raw data in the Flevoland test area and a simulated point target like the real one shown in Fig. 3. All algorithms process 6 looks in azimuth and range getting a decimation factor around 8 in range and around 40 in azimuth. The Integrated Side Lobe Ratio (ISRL) is obtained from the response of a simulated point target, and the Equivalent Number of Looks (ENL) is obtained from the analysis of a uniform area of the processed SAR image (see Figs. 4 and 5). Another value used for comparison in Table I is the spatial resolution. The CZT-SPECAN gives very sharp impulse response at the cost of worse values for ENL and ISRL. However, the flexibility given by this technique is very interesting for on-board implementations as shown in [4]. The conclusion obtained from this study is that

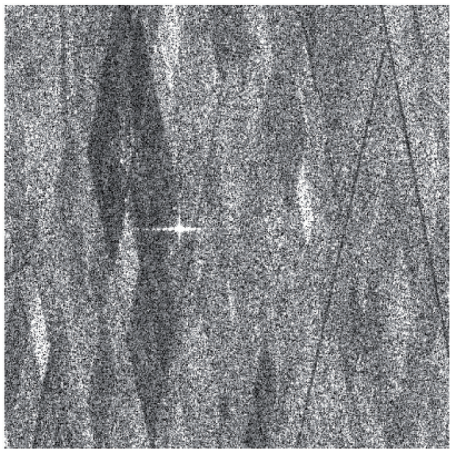

Figure 3. *Point target in a one look ERS-1 SAR image processed with the Chirp Scaling Algorithm.*

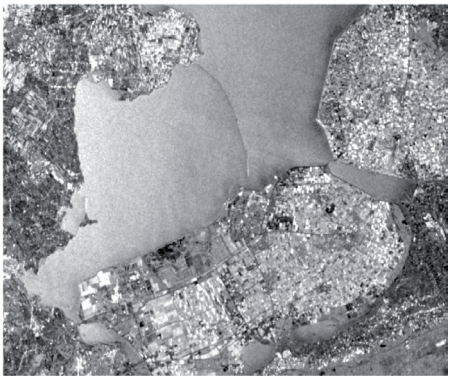

Figure 4. *Test area processed with a high number of looks (484) and the Range-Doppler algorithm.*

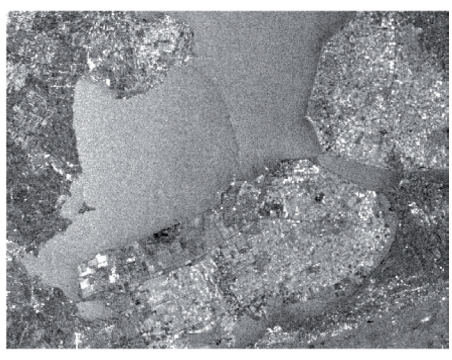

Figure 5. *Test area image processed with CZT SPECAN using 6 looks in both range and azimuth dimensions.*

The Discrete Wavelet Transform has the property of simultaneous space and frequency localization.

SPECAN and especially SPECAN combined with Chirp-Z Transform is a very appropriate candidate for processing SAR data not only in azimuth but also in range. These new developments are very promising for obtaining fast and simple SAR image generation and they could be suitable candidates for potential on-board implementation.

4. Speckle Noise

One of the main drawbacks in Synthetic Aperture Radar (SAR) image exploitation and application development is caused by the presence of noise. SAR images contain several sources of noise. In addition to the thermal noise given by electronic equipment, there is another kind of distortion that is typical in SAR systems. It is called Speckle noise, in parallelism with a similar effect that appears in laser imaging (see [8] and [9]). The relatively narrow bandwidth combined with the surface roughness at the wavelength scale produce a pattern of interference that results in a grainy appearance as explained in [2]. Noise affects severely post-processing applications like segmentation and classification, and its effect can be seen in Fig. 3 where a one look SAR image is shown.

Many methods that reduce Speckle noise while preserving texture and detail have been presented in the literature. In this study, a comparison of different methods using Wavelet decomposition is performed and new improvements for traditional methods are introduced (see [10] and [11]). These techniques are: Wiener filtering, classical soft threshold, and an adaptive soft threshold. The last method combines the characteristics of additive noise reduction of soft thresholding (see [12] and [13]) with the localization of information in the coarsest levels of the Wavelet transform (see [14] and [15]), and its main contribution is to adapt the effective threshold to the level of decomposition.

The noise reduction process is summarized in Fig. 6. The scheme is the same that was introduced by Donoho in [12] with the logarithmic operation proposed by Odegard in [13]. The novelty here is introduced in an adaptive version of the threshold implementation. The logarithmic transformation is applied in order to separate the noise contribution from the desired signal in an additive manner. Then, the image is decomposed via the Discrete Wavelet Transform using a three level pyramid with Daubechies family of 16th order as described by Daubechies in [14]. This wavelet is widely used because it provides compactly supported orthonormal bases, and it may be implemented efficiently with a tree filtering scheme that creates a pyramid of lower resolution approximations.

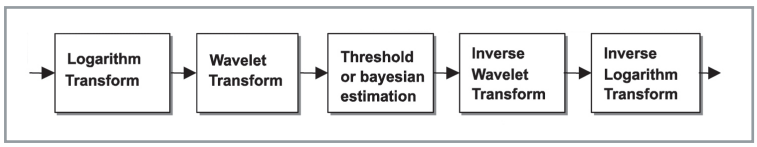

Figure 6. *Speckle noise reduction scheme.*

The Discrete Wavelet Transform has an interesting property of simultaneous space and frequency localization. For that reason, the features are present through the decomposition tree. Therefore, such detail information may be kept and noise can be reduced by applying a threshold detector that does not produce edge distortion. An illustration of the 2-D discrete Wavelet decomposition is shown in Fig. 7.

The technique called soft thresholding is then applied to reduce additive Gaussian noise in the Wavelet domain of the logarithmically transformed image. In general, one of the key aspects in thresholding is the choice of the threshold value. This is the most critical step in the Wavelet shrinkage operation, since a poor adjustment may provide a distorted image or unnoticeable noise reduction. The innovation to standard algorithm is a two-fold modified shrinkage operation. First, coefficient processing is carried out independently in each detail sub-image, and only the sub-image coefficients are taken into consideration for the computation of the standard deviation. Secondly, the design parameter is not constant but dependent on the level of decomposition.

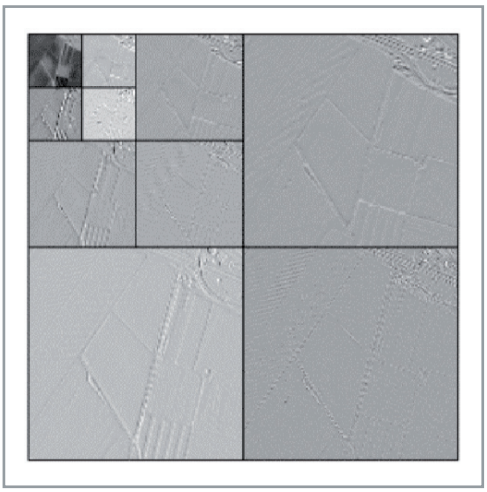

Figure 7. *Wavelet transformed original image.*

The first step is to analyze the statistics of Speckle noise in SAR images. Then, a simulated image following these characteristics is created using a noise-free optical image in order to evaluate properly noise reduction. The mean square error is classified depending on the spatial characteristics of a local region, and this tool gives valuable information for algorithm assessment. In the comparison, the new adaptive soft threshold method provides excellent results concerning noise reduction and detail preservation compared to classical soft threshold and the Wiener filter. Besides, it gives as much noise reduction as the

most sophisticated Bayesian method (see [11]), but much more efficiently. So, the adaptive version of soft thresholding outperforms the other techniques. Figure 8 summarizes the algorithm performance of these three techniques applied to a simulated SAR image following the Speckle statistics with a signal to noise ratio equal to 20 dB. It shows the best results in edge error cancellation in relation to the achieved uniform error cancellation, whereas Fig. 9 presents the noise-free image, the simulated SAR image and the restored image using the adaptive technique.

5. Optical remote sensing and data fusion

This section covers the Remote Sensing activities concerning classification and change detection using optical data and it also proposes the use of SAR data to help the previous processes through data fusion. SAR data may complement the optical higher resolution images by enhancing the detection of man-made targets and soil moisture. These are the most interesting features of SAR data, and they may be incorporated in the optical classification algorithms.

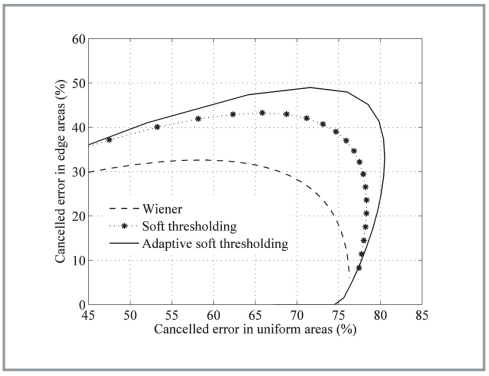

Figure 8. *Comparison of best mean square error cancellation in edge areas and uniform areas.*

The geographical region of study is the Vinalopó river basin, in the province of Alicante in the East coast of Spain, and the main objectives have been crop and irrigation detection for water management and monitoring of illegal constructions. The agricultural characteristics of the zone present an important challenge for classification algorithms due to the irregular irrigation practice throughout the year and the small size of the parcels. Another challenge in crop classification in that area comes in the form of mixed crops. The main crops in the Vinalopó region are olive trees and vineyards (both irrigated and non-irrigated). The use of water for crop irrigation is a very important indicator for water management agencies. In Spain, water shortage is a very severe problem and water usage needs to be strictly controlled. An alternative to the ground campaigns comes from the use of a classification method with satellite multispectral images. This kind of data is consistent and systematically acquired using the same sensor. By using such satellite data, field work can not be eliminated but it is reduced to a minimum. Therefore, monitoring campaigns are less expensive in economic and time costs.

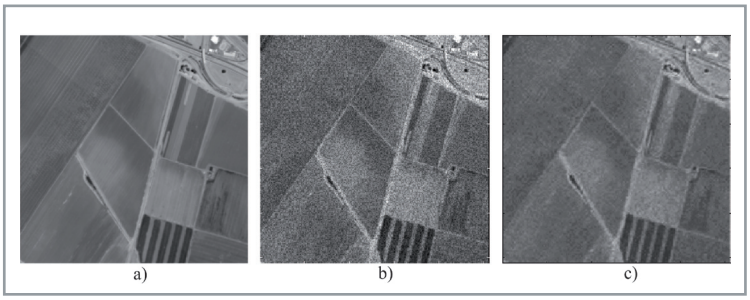

Figure 9. *Original noise-free image in a), simulated speckled image in b) and restored image with the adaptive soft thresholding method in c).*

In this section, three main optical data sources are employed. The first one is the ASTER instrument onboard the TERRA spatial platform, whose characteristics have been described in the Introduction (the VNIR sensor in 15 m of pixel spacing and the SWIR sensor at 30 m of pixel spacing). ASTER data is chosen due to the wide spectral range and the relatively high spatial resolution. The second source of information is orthorectified aerial image in the Red Green and Blue (RGB) bands. The aerial image presents 0.5 m of pixel size and it would be very similar to the commercial satellite high resolution products (see an example in Fig. 10). The third source of information is the TerraSAR-X stripmap product (pixel spacing of 1.5 m) to introduce the data fusion using SAR data. This satellite product presents a spatial resolution which is comparable to the high resolution commercial imagery in the submeter range. Some additional data coming from ground truth has been used and the parcel boundaries from cadastral information have been also available.

6. Image classification for crop and irrigation identification

The ability to distinguish between land cover classes is closely related to their growing patterns, and there are several periods when different land cover categories have a similar spectral response. Therefore, it is possible to misclassify

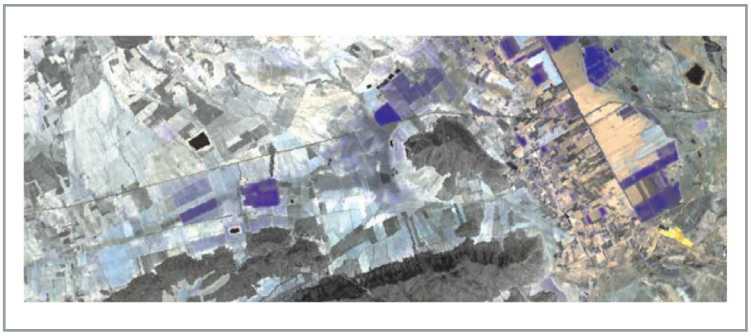

Figure 10. *ASTER VNIR image of an area of Villena.*

SAR data may complement the optical higher resolution images by enhancing the detection of man-made targets and soil moisture.

different land covers if only a single date image is used. In order to overcome this problem, several images of different dates are employed, thus improving the accuracy of the classification.

Different methods for multi-temporal crop classification have been developed before in some regions of Spain using Landsat images (see [16] and [17]). However, the different techniques should be adapted and modified to satisfy the requirements of the specific campaign and the particular characteristics of the crops and irrigation methods of the area under analysis. A comparison among multi-temporal classification methods using ASTER data was previously presented by the authors in [18] and [19] in the region of Novelda (Vinalopó basin).

The classification process is carried out in different steps, once the satellite images are selected. First, geometric and radiometric data correction is needed with the purpose of eliminating any possible image anomaly including cloud and atmospheric artifacts. Several radiometric correction methods based on relative techniques have been tested and the best one has been selected. The selected method is based on the minimization of the differences between pixels that are considered as invariant through the images. In our study, an adaptation of the no-change Simple Regression (see [20]), which basically substitutes the simple Least Squares Regression by a Mean-Standard Deviation technique, has been carried out. Then, a non-supervised classifier is used in order to identify spectrally pure regions that are used to train the supervised classifier. Some ground observations are needed at this point in order to properly define the training regions and to choose the final classes in the legend.

Several supervised multi-temporal classification methods including change detection have been compared and presented in [19]. The sequential masking method proposed in [21] has been also implemented and evaluated. Finally, two methods based on change detection coming from image differences and image quotients have been also carried out. The best performance is given by the simplest method that treats different dates as extra bands and applies a majority filter after classification. Finally, a thematic map obtained from the best algorithm obtained is shown in Table II and its legend in Table III. Some classes like water are very well characterized, but some others like the irrigated arable lands present poor results.

CLASS	WA	IM	FY	VY-I	VY	AL	PR	AL-I	UC	OR-I	OR	TOTAL
WA	100.00	0.00	0.00	0.00	0.07	0.00	0.00	0.00	0.00	0.00	0.00	0.49
IM	0.00	64.62	0.00	0.00	0.00	0.00	0.00	0.00	0.00	0.00	0.00	0.57
FY	0.00	0.00	90.52	2.89	2.76	0.13	0.00	41.04	0.00	0.00	0.00	9.69
VY-I	0.00	0.00	1.52	91.70	39.94	0.13	0.48	11.94	0.00	1.28	28.30	43.46
VY	0.00	16.92	3.55	3.99	47.62	4.44	15.40	14.93	13.79	29.49	28.30	14.38
AL	0.00	6.15	2.54	0.57	1.94	89.85	3.97	13.43	0.00	0.00	0.00	19.62
PR	0.00	12.31	0.85	0.18	7.26	3.36	80.16	11.94	0.00	15.38	0.00	9.60
AL-I	0.00	0.00	1.02	0.68	0.14	2.08	0.00	6.72	0.00	7.69	0.00	0.99
UC	0.00	0.00	0.00	0.00	0.00	0.00	0.00	0.00	86.21	0.00	0.00	0.34
OR-I	0.00	0.00	0.00	0.00	0.00	0.00	0.00	0.00	0.00	46.15	0.00	0.49
OR	0.00	0.00	0.00	0.00	0.28	0.00	0.00	0.00	0.00	0.00	43.40	0.37
TOTAL	100.00	100.00	100.00	100.00	100.00	100.00	100.00	100.00	100.00	100.00	100.00	100.00

Table II. *Confusion matrix (%).*

Other classification algorithms based on classical algorithms (see [23]) and learning processes like Artificial Neural Networks and Support Vector machines were also implemented and tested. They offer very good results at a more elevated cost in implementation and operator time.

7. Image classification for irrigation detection using a priori crop information

The classification results using multi-temporal ASTER data working on a "per pixel" basis present some important drawbacks. The sensor has shown an interesting property to detect irrigation, especially if a dry season image is used, since non-irrigated vegetation presents severe stress due to lack of water. However, pixel spacing coming from ASTER is too small for the typical parcel size in the zone. Nevertheless, the typical crop in this area is olive tree, vineyard and fruit tree. All these are long-term crops and they usually remain through the years.

WA	Water
IM	Improductive
FY	Frutal tree
VY-I	Vineyard (irrigated)
VY	Vineyard (non irrigated)
AL	Arable land (non irrigated)
PR	Shrub-like pasture
AL-I	Arable land (irrigated)
UC	Under cover vineyard (irrigated)
OR-I	Orchard (irrigated)
OR	Orchard (non irrigated)

Table III. *Legend for Table II.*

Then, crop classification could be done in two steps. First, the type of crop could be obtained performing segmentation on high resolution data (RGB aerial image) disregarding the irrigation (see Fig. 11). Secondly, an irrigation study taking into account the previous crop information could be performed continuously using ASTER data (VNIR and SWIR sensors). The procedure is similar to the crop classification described in the previous section, but only two classes must be detected now: irrigated and non-irrigated crop. The irrigation detection is carried out with each crop type, and afterwards post-classification procedures like parcel integration may be performed.

The final global classification is shown in Fig. 12 b) compared with the ground truth in Fig. 12 a). The results, shown in Fig 12 and Table IV, are very successful and they may be repeated systematically, since the irrigation information is coming from the ASTER satellite acquisition that is much more flexible and systematic than the aerial image that is used for segmentation and classification of crop type in each parcel.

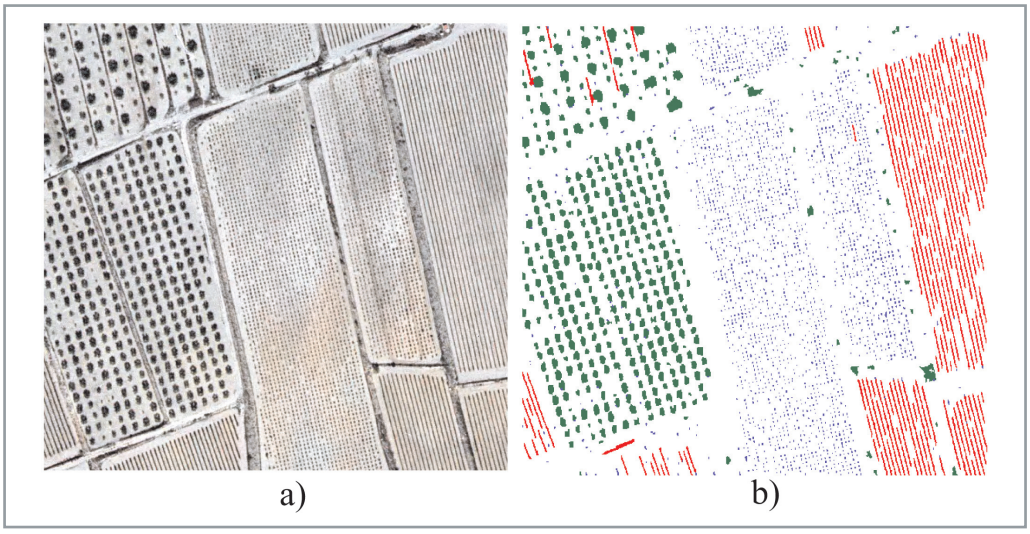

Figure 11. *Aerial image of a crop area in Villena in a) and a segmentation crop classification in b).*

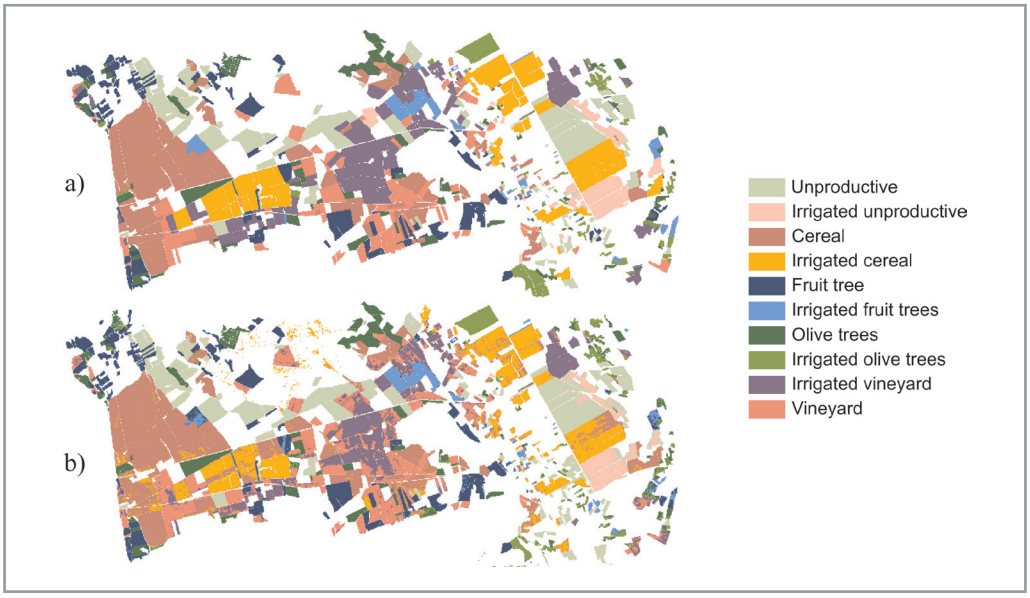

Figure 12. *Classification in Villena area: ground truth in a) and two-step classification results in b).*

Crop	Accuracy (%)
Vineyard	81.20
Olive trees	91.61
Cereal	91.24
Unproductive	84.96

Table IV. *Accuracy in the detection of irrigation in an area of Villena.*

8. Change detection and data fusion

The detection of man-made constructions using high resolution images is an interesting application for governments and town councils. The change detection for the search of illegal building work may be carried out using high resolution data and a segmentation process. In Fig 13 a) we show the original aerial image with 0.5 m of pixel size. Fig 13 b) shows the classification after segmentation in search of man-made constructions and swimming pools. Fig. 13 c) shows the same scene from TerraSAR-X SAR data at 1.5 m pixel size. In this case, the SAR image is not very clear, only the roads and some buildings are visible with very low and very high values of backscattering values respectively. However, this data may be of interest to help the segmentation and classification process that may be very complicated when the building roofs somehow coincide in the visible range with the surrounding soil.

Another comparison between optical and SAR data is presented in Fig. 14. In this case, the city centre of Villena is imaged with aerial RGB data (0.5 m of pixel size) and TerraSAR-X data (1.5 m of pixel size). Now, the building structure is much more visible in the SAR image, and this could contribute to help the segmentation and classification algorithms working on high resolution RGB data.

The detection of man-made constructions using high resolution images is an interesting application for governments and town councils.

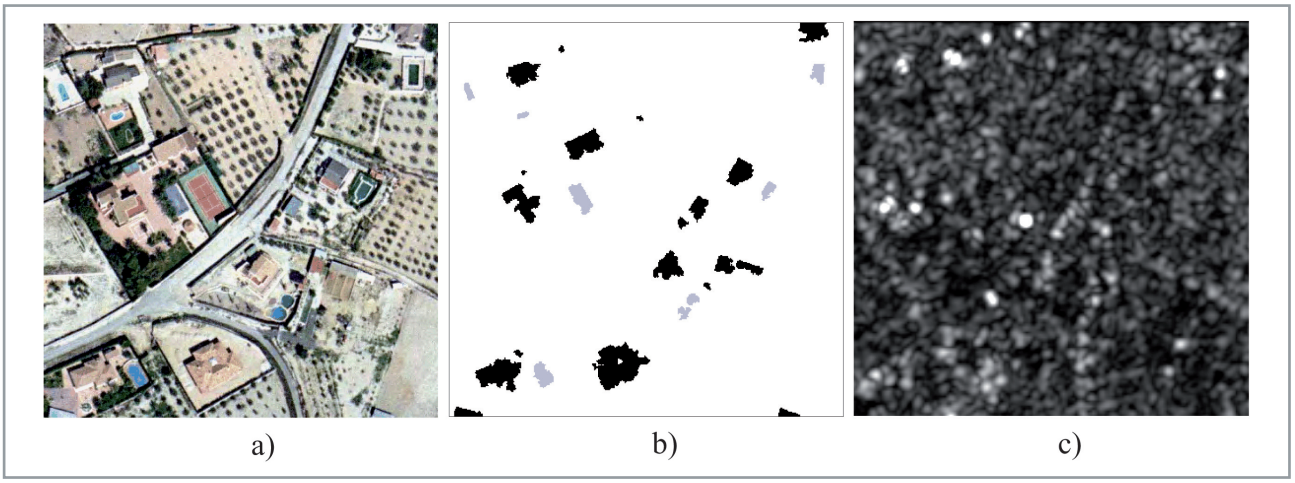

Figure 13. *Optical image in a), classification showing buildings and swimming-pools in b) and SAR scene in c).*

9. Conclusions

This paper presents the current and near future activities developed by the Microwave Applications Group GAM, within the *Instituto de Telecomunicaciones y Aplicaciones Multimedia* (iTEAM). Research lines related to SAR image formation and optical data interpretation for various purposes have been presented; the selected applications have been crop classification, irrigation detection and change detection in search for illegal constructions. The deployment of accurate and precise new sensors on board spatial platforms using optical and microwave frequencies paves the way for a wide variety of new applications that users are demanding increasingly. Promising results using per object classification with aerial ortho-rectified imagery could be improved by an intelligent combination of SAR data and submeter resolution satellite images.

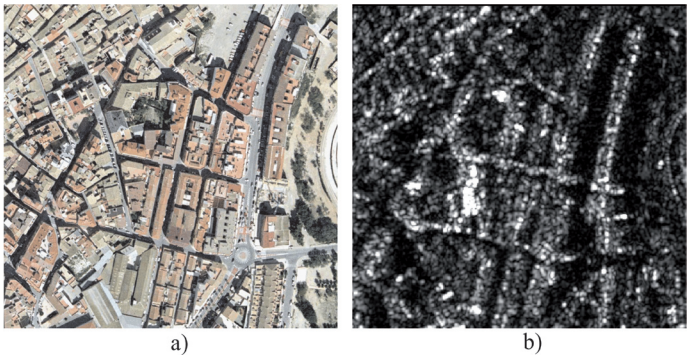

Figure 14. *Aerial RGB image in a) and TERRASAR-X image in b) of an area of Villena city centre.*

Acknowledgments

The authors want to thank the European Space Agency and the German Aerospace Center for the provision of ERS and TERRASAR-X data, respectively. The authors also want to thank *Confederación Hidrográfica del Júcar*, which has provided the data and the funding for some of the described activities.

References

[1] E. Chuvieco, Teledetección ambiental: La observación de la Tierra desde el espacio. Ariel, 2008.

[2] J. C. Curlander and R. McDonough, Synthetic Aperture Radar Systems and Signal Processing. John Wiley and Sons Inc., 1991.

[3] K. L. Liu and W. E. Arens, "Spacecraft on-board SAR image generation for EOS-type missions", IEEE Transactions on Geoscience and Remote Sensing, vol. 27, no. 2, pp. 184-192, 1989.

[4] A. Vidal and M. Ferrando, "On-Board medium resolution SAR processing for fast image generation", International Journal of Remote Sensing, vol. 25, pp. 161-176, 2004.

[5] A. Vidal-Pantaleoni, R. Oviol, and M. Ferrando, "A comparison of phase unwrapping techniques in Synthetic Aperture Radar Interferometry", in Proc. IGARSS'99, pp. 1354-1356, 1999.

[6] A. Vidal-Pantaleoni and M. Ferrando, "A new spectral analysis algorithm for ScanSAR and medium resolution SAR data processing without interpolation", in Proc. IGARSS'98, pp. 639 -641, 1998.

[7] A. Vidal-Pantaleoni and M. Ferrando, "A comparison of SAR processing SPECAN techniques for efficient ScanSAR image generation", in Proceedings of the SPIE vol. 3497, pp. 31-42, 1998.

[8] H. H. Arsenault and G. April, "Properties of Speckle integrated with a finite aperture and logarithmically transformed", Journal of the Optical Society of America, vol. 66, no. 11, pp. 1160-1163, 1976.

[9] J. C. Dainty, Laser Speckle and Related Phenomena. Springer-Verlag, 1984.

[10] A. Vidal-Pantaleoni, D. Martí, and M. Ferrando, "An adaptive multiresolution method for speckle noise reduction in synthetic aperture radar images", in Proc. IGARSS'99, pp. 1325-1327, 1999.

[11] A. Vidal and D. Martí, "Comparison of different Speckle reduction techniques in SAR images using Wavelet transform", International Journal of Remote Sensing, vol. 25, pp 4915-4932, 2004.

[12] D. L. Donoho, "De-noising by Soft Thresholding", IEEE Transactions on Information Theory, vol. 41, pp. 613-627, 1995.
[13] J. E. Odegard, H. Guo, M. Lang, C. S. Burrus, R. O. Wells, L. M. Novak, and M. Hiett, "Wavelet-based SAR Speckle reduction and image compression", Proceedings of the SPIE, vol. 2487, pp. 259-271, 1995.
[14] I. Daubechies, "Orthonormal Bases of Compactly Supported Wavelets", Communications on Pure Applied Mathematics, vol. 441, pp. 909-996, 1988.
[15] M. Simard and G. DeGrandi, "Analysis of Speckle Noise Contribution on Wavelet Decomposition of SAR Images", IEEE Transactions on Geoscience and Remote Sensing, vol. 36, no. 6, pp. 1953-1962, 1998.
[16] J. P. Guerschman, J. M. Paruelo, C. Di Bella, M. C. Giallorenzi, and F. Pacin, "Land cover classification in the Argentine Pampas using multitemporal Landsat TM data", International Journal of Remote Sensing, vol. 24, pp. 3381-3402, 2003.
[17] A. Calera, J. Reyes, C. Martínez, and J. Sánchez, "Seguimiento de los cultivos de regadío en la mancha oriental desde 1982 a 1997, utilizando imgenes TM y MSS, en combinación con herramientas SIG", Revista de Teledección, pp. 57–61, 1999.
[18] B. Hoyos, M. Hidalgo, and A. Vidal, "Evaluation of multi-temporal methods for crop classification using ASTER images", Proc of the II Recent Advances in Quantitative Remote Sensing, pp. 670-675, 2006.
[19] M. Llopis, A. Vidal, and B. Hoyos, "Multi-temporal classification for irrigation detection in the Vinalopo region in Spain using ASTER images", in Proc. IGARSS'07, pp. 3659-3662, 2007.
[20] D. Yuan and C. D. Elvidge, "Comparison of relative radiometric normalization techniques", ISPRS Journal of Photogrammetry and Remote Sensing, vol. 51, pp. 117–126, 1996.
[21] M. Arikan, "Parcel-based crop mapping through multi-temporal masking classification of Landsat 7 images in Karacabey, Turkey", The International Archives of the Photogrammetry, Remote Sensing and Spatial Information Sciences, vol. 34, 2003.
[22] E. Rubio, M. M. Artigao, V. Caselles, C. Coll, and E. Valor, "Cartografiado de la vid con datos Landsat-TM. aplicación a una zona de Tomelloso (Ciudad Real)", Revista de Teledección, vol. 15, pp. 47–56, 2001.
[23] B. Hoyos, S. López, A. Vidal, and M. Ferrando, "Clasificación de cultivos en parcela pequeña en la zona del Vinalopó mediante imágenes ASTER", Actas del Congreso Nacional de Teledetección, 2005.

Biographies

Ana Vidal Pantaleoni was born in Valencia, Spain in 1970. She received the Ingeniero de Telecomunicación degree from the Universidad Politécnica de Valencia, Valencia, Spain, in 1993. She spent one year at University of Strathclyde (Glasgow, Scotland, 1993) thanks to the Erasmus international exchange program. In 1993, she became a Research Assistant in the Universidad Politécnica de Valencia. In 1995 and 1996 she was held a Spanish Trainee position with the European Space research and Technology Centre (ESTEC)-European Space Agency (ESA), Noordwijk, the Netherlands, where he was involved in the study and implementation of software for Synthetic Aperture Radar (SAR) image processing. In 1996 she went back to the Universidad Politécnica de Valencia, where she held several lecturing positions, and she became Associate Professor in 2001. Her current interests are SAR data processing, SAR Speckle noise reduction and numerical methods based on Wavelet transform for microwave structure analysis.

Berta Hoyos Ortega was born in Albacete, Spain, on August 25, 1980. She received the Ingeniero de Telecomunicacion degree from the Universidad Politecnica de Valencia (UPV) in 2005, and she is currently working at the European Space Agency based at ESTEC (in Noordwijk, The Netherlands) as Commissioning and Post Launch Support Engineer. From 2004 to 2006, she was a Fellow Researcher working in satellite data classification within the GAM research group (iTEAM, UPV). From 2006 to 2008, she has been a Fellow Researcher at ESTEC in the field of Radar Altimeters, in particular of ERS-2 and ENVISAT, at the Post Launch Support Office. Her current research interests are satellite payloads and satellite image processing.

Mercé Llopis Ferrer was born in Paiporta, Valencia, Spain, on February 26, 1982. She received the Ingeniero de Telecomunicación degree from the Universidad Politécnica de Valencia, Valencia, Spain, in 2007. She spent one year at University of Hannover (Germany, 2006) thanks to Erasmus international exchange program. In 2007-2008, she was a Fellow Research

with the GAM (iTEAM, UPV) working on Artificial Neural Networks for satellite image classification. From March 2008 to November 2008 she was in the Institut de Ciències de l'Espai de Catalunya where she developed the Acquisition Data System of a CdTe detector of Gamma ray. Currently, she is working in the Defence Ministry of Spain with Earth Observation operations.

Mariola Montoliu Fortuño was born in Vila-real, Castellon, Spain, on October 25, 1982. She received the Telecommunications Engineering Degree from the Universidad Politécnica de Valencia (UPV), Valencia, Spain in 2007. She carried out her Final Year Project and she was a Fellow Researcher at the GAM group (iTEAM, UPV), where her work was focused in crop classification using ASTER satellite image and ground truth data. She is currently working at the Spanish company AWA in wireless network design and maintenance.

Mª Rocío Moreno Cambronero was born in Valencia in 1982. She is studying at the Universidad Politecnica de Valencia to get the Telecommunications Engineering Degree. She is currently carrying out her Final Year Project in the GAM (iTEAM, UPV), in the area of image classification for Earth Observation.

Máriam Taroncher (S'03) was born in Lliria, Valencia, Spain, on October 8, 1979. She received the Telecommunications Engineering degree from the Universidad Politécnica de Valencia (UPV), Valencia, Spain, in 2003, and she is currently working toward the Ph.D. degree at UPV. From 2002 to 2004, she was a Fellow Researcher with the UPV. Since 2004, she has been a Technical Researcher in charge of the experimental laboratory for high power effects in waveguide devices at the Research Institute iTEAM, UPV. In 2006 she was awarded a Trainee position at the European Space Research and Technology Centre, European Space Agency (ESTEC-ESA), Noordwijk, The Netherlands, where she worked in the Payload Systems Division Laboratory in the area of Multipactor, Corona Discharge and Passive Intermodulation (PIM) effects. Her current research interests include numerical methods for the analysis of waveguide structures and the acceleration of the electromagnetic analysis methods.

Vicente E. Boria Esbert received the Ingeniero de Telecomunicación and the Doctor Ingeniero de Telecomunicación degrees from the Universidad Politécnica de Valencia, Valencia, Spain, in 1993 and 1997, respectively. In 1993 he joined the Departamento de Comunicaciones, Universidad Politécnica de Valencia, where he is Full Professor (since 2003). In 1995 and 1996 he was held a Spanish Trainee position with the European Space research and Technology Centre (ESTEC)-European Space Agency (ESA), Noordwijk, the Netherlands. Since 2003, he has served on the Editorial Boards of the IEEE Transactions on Microwave Theory and Techniques. He is also member of the Technical Committees of the IEEE-MTT International Microwave Symposium and of the European Microwave Conference. His current research interests include numerical methods for the analysis of waveguide and scattering structures, automated design of waveguide components, radiating systems, measurement techniques, and power effects in passive waveguide systems.